

canopy, the forward scattering of the trunk layer shows great influence on the scattering properties of the forest. Applying the approximate analytical solutions for the first-order and second-order scattering fields obtained above, the variations of the forward scattering cross sections of two adjacent conducting cylinders and dielectric cylinders via the incidence angles are calculated in this paper. To verify the validation, the scattering results are compared with those obtained by using the Numerical Electromagnetic Code (NEC), which is a computational package based on the moment method, and only those of conducting cylinders are compared because the version of NEC we have only provides for metallic objects.

Suppose the length of cylinders is 18 cm and the radius is 0.2 cm. The conducting cylinder is perfect, and the relative dielectric constant of dielectric cylinder is (9.6, $j4.0$). The frequency of the excitation wave is 9.6 GHz, and the incident plane-wave is arranged in $x-z$ plane, i.e., the azimuthal incidence angle is 180° .

Figs. 2 and 3 give the VV-polarized azimuthal patterns of forward RCS for two conducting cylinders when the elevation incidence angle is 35° . In Fig. 2, the position of the second cylinder is $(\tilde{\rho}, \tilde{\phi}) = (18 \text{ cm}, 180^\circ)$. In this case, the two cylinders are located far enough apart that the secondary scattering shows very little effect. The first- and second-order scattering results are all in agreement with the moment-method computation results. In Fig. 3, the two cylinders are relatively close and the position of the second cylinder is $(\tilde{\rho}, \tilde{\phi}) = (2.5 \text{ cm}, 180^\circ)$. It may be seen that the second-order scattering result is in agreement with the moment method data and provides a reasonable approximation.

Figs. 4 and 5 give the VV-polarized elevation patterns of forward RCS for two conducting cylinders when the azimuthal scattering angle is $\phi_s = 0^\circ$. The position of the second cylinder is $(\tilde{\rho}, \tilde{\phi}) = (4 \text{ cm}, 180^\circ)$ in Fig. 4 and 8 cm, 180° in Fig. 5. The peak in the first-order scattering results is due to the constructive interference of scattering fields from two cylinders and may be decreased significantly by the inclusion of the secondary scattering terms. From these two figures, we can see that the difference between the first- and second-order results increases with the incidence angle except in the interference peak. This is because the angle of the primary forward scattering cone becomes larger when the incidence angle increases, and this leads to the increment of the secondary scattering length $L1$. The HH-polarized results are not given for the reason that the values of HH-polarized RCS of conducting cylinders are small, and, therefore, the effect of the secondary scattering is small.

For two dielectric cylinders, the VV- and HH-polarized elevation patterns of forward RCS, which also show the differences between the first- and second-order scattering results, are given in Figs. 6 and 7. In Fig. 6, the position of the second cylinder is $(\tilde{\rho}, \tilde{\phi}) = (4 \text{ cm}, 180^\circ)$, and in Fig. 7 it is (4 cm, 90°). From these figures, we can see that the secondary scattering has a greater effect on VV-polarized response than HH-polarized response.

IV. CONCLUSIONS

The closed-form solution of the scattered field up to second order from two adjacent finite length cylinders has been obtained in this paper based on the reciprocity theorem. Its validity was verified by comparing analytical results with method of moments computations, and agreement was obtained. The results show that the secondary scattering due to interaction between the two cylinders has some effects on the scattered field. The present work should provide

a theoretical basis for the simulations of forest canopy scattering considering the effect of multiple scattering between trunks.

REFERENCES

- [1] M. A. Karam and A. K. Fung, "Electromagnetic scattering from a layer of finite-length, randomly oriented dielectric circular over a rough interface with application to vegetation," *Int. J. Remote Sensing*, vol. 9, no. 6, pp. 1109–1134, 1988.
- [2] M. K. Karam, A. K. Fung, R. H. Lang, and N. S. Chauhan, "A microwave scattering model for layered vegetation," *IEEE Trans. Geosci. Remote Sensing*, vol. 30, pp. 767–784, July 1992.
- [3] K. Sarabandi and P. F. Polatin, "Electromagnetic scattering from two adjacent objects," *IEEE Trans. Antennas Propagat.*, vol. 42, pp. 510–516, Apr. 1994.
- [4] K. Sarabandi, P. F. Polatin, and F. T. Ulaby, "Monte Carlo simulation of scattering from a layer of vertical cylinders," *IEEE Trans. Antennas Propagat.*, vol. 41, pp. 465–474, Apr. 1993.
- [5] G. T. Ruck, D. E. Barrick, W. D. Stuart, and C. K. Krichbaum, *Radar Cross-Section Handbook*. New York: Plenum, 1970, pp. 272–274.

Polarimetric SAR Imaging of Buried Landmines

Lawrence Carin, Ravinder Kapoor, and Carl E. Baum

Abstract—If the fields incident on a buried body of revolution are polarized vertically or horizontally (relative to the ground), the backscattered fields are exclusively copolarized (i.e., there are no cross-polarized backscattered fields). After substantiating this theoretically, measured ultrawideband (UWB) synthetic aperture radar (SAR) data are used for corroboration, considering real, buried landmines that approximate bodies of revolution.

Index Terms—Ground-penetrating radar (GPR), polarization, synthetic aperture radar (SAR).

I. INTRODUCTION

Over the last several decades, ground-penetrating radar (GPR) has been an important tool for buried-target detection and identification [1]–[3]. In most GPR systems, the antenna is placed on or near the ground, such that the buried target is generally in the near zone of the often complicated antenna pattern. Since the fields incident on the target are usually not polarized simply (especially as the target-sensor orientation varies), polarimetric processing is difficult. Alternatively, there has been recent interest in synthetic aperture radar (SAR) for buried-mine detection [4], [5]. Such systems offer the advantage of a significant standoff distance; moreover, since the targets are in the far zone of the source, relatively simple antenna designs can realize linearly polarized incident fields. While a SAR system may have difficulty detecting all individual mines, it can be an effective tool for mine-field detection, after which conventional GPR, electromagnetic

Manuscript received October 21, 1997; revised December 8, 1997.

L. Carin is with the Department of Electrical and Computer Engineering, Duke University, Durham, NC 27708-0291 USA (e-mail: lcarin@ee.duke.edu).

R. Kapoor is with the Army Research Laboratory, AMSRL-SE-RU, Adelphi, MD 20783 USA.

C. E. Baum is with Phillips Laboratory, Kirtland AFB, Albuquerque, NM 87117-5776 USA.

Publisher Item Identifier S 0196-2892(98)05625-3.

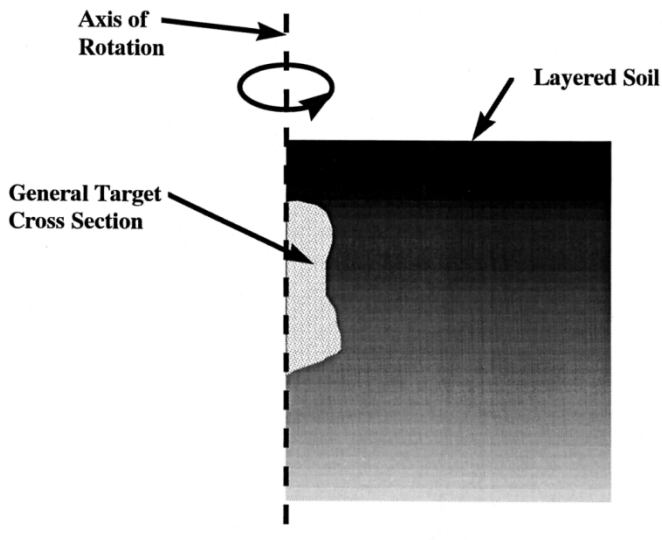


Fig. 1. Schematization of a general body of revolution.

induction (EMI), magnetometers, or other local sensors [6], [7] can be employed.

Given that a SAR system affords the potential for polarimetric detection of buried mines, in this letter, we explore this issue by considering a special but important class of land mines. In particular, we assume that the mine and the background media can be modeled as a body of revolution (BOR), implying that the buried mine and its surrounding environment can be modeled approximately by rotating a general two-dimensional (2-D) profile about an axis (see Fig. 1). A special case of such is a BOR target buried in a half space, with the BOR axis perpendicular to the air-ground interface [8]–[10]; more generally, the soil can be layered, discretely or continuously. Finally, note that the BOR mine can be metal, dielectric, or a combination of both, although the measured data considered here are restricted to the case of metal mines.

We assume that the target-sensor distance is large, such that the fields incident on the target are characterized by either a vertically or horizontally polarized plane wave, incident obliquely. For this special class of BOR targets, a symmetry plane is defined by the rotation axis and the line connecting the target center and the sensor. Since the incident plane wave satisfies symmetry properties about this plane, and because the target is symmetric about the same plane, the scattered fields will satisfy symmetry properties [11], [12]. In particular, if the incident fields are vertically polarized, the incident electric fields on either side of the symmetry plane are identical and, therefore, the same is true of the scattered electric fields; this constraint is satisfied if and only if the backscattered fields (in the plane of symmetry) are vertically polarized. There are therefore no cross-polarized backscattered fields. However, note that such symmetry does not imply that the *bistatic* fields are vertically polarized, only that at angles $\pm\theta$ from the symmetry plane the bistatic fields are polarized identically, with respect to this plane. Using the same logic, if the incident fields are horizontally polarized, the backscattered fields are as well. Therefore, in summary, for this special but important class of buried targets, the cross-polarized (VH and HV) fields are zero in the backscatter direction. The above polarimetric properties apply to any discretely or continuously layered soil profile, and they can be confirmed through consideration of the Green's functions for special cases (e.g., the half-space problem [8]–[10]).

In most SAR systems, the fields are measured in backscatter for a particular sensor position, along what subsequently becomes



Fig. 2. The M20 anti-tank mine used in the measurements (the ruler indicates 30.48 cm).

a synthetic aperture. Therefore, we expect the above polarimetric properties to manifest themselves in actual SAR imagery. This therefore provides an important and, to our knowledge, new tool for discriminating a ubiquitous class of mines from natural clutter (e.g., rocks, roots, etc.) that generally do not satisfy the BOR model. To demonstrate the potential of such a discrimination strategy, we consider polarimetric SAR imagery measured for an anti-tank mine, the “M20” shown in Fig. 2. The M20 mine was placed on the soil surface and buried at a depth of 6 in, although space constraints restrict the results presented here to the buried case. Upon conclusion, we discuss our experience with the surface mines and a class of anti-personnel mines.

The measurements were performed at Yuma Proving Grounds, Yuma, AZ (USA), with the data collected using an ultrawideband (UWB), time-domain radar [4]. In short, the radar transmits a pulse with bandwidth from approximately 50 to 1200 MHz. The radiation is effected via flared, parallel-plate horn antennas, which, over a relatively large beamwidth, emit nearly pure linearly polarized radiation. Four antennas are employed: vertically and horizontally oriented transmit antennas as well as vertical and horizontal receive antennas. Although the measurements are therefore not strictly backscatter, the distance between the four antennas is inconsequential relative to the target-sensor distance. The four antennas are placed atop a boom lift, 150 ft above the ground, and the entire unit is driven to effect a synthetic aperture. The mines are placed in the ground using military doctrine, and the region under consideration is contaminated by rocks, desert vegetation, and animal burrows. Every attempt is made to make the field under test as close as possible to what would be expected in an actual minefield (i.e., these are not sandbox-type experiments).

The measurements are performed in the time domain, and the SAR image is formed via a simple “delay-and-sum” procedure [4], utilizing the speed of light. We produce four images, one for each polarization (VV, HH, HV, and VH). We have considered many buried and surface mines, with the results presented here representative. The SAR imagery (Fig. 3) clearly demonstrates that the copolarized (VV and HH) target images are large relative to their cross-polarized (HV) counterparts. In the HV image, the sequence of mines (identified by arrows in the HH and VV images) are virtually invisible. While such

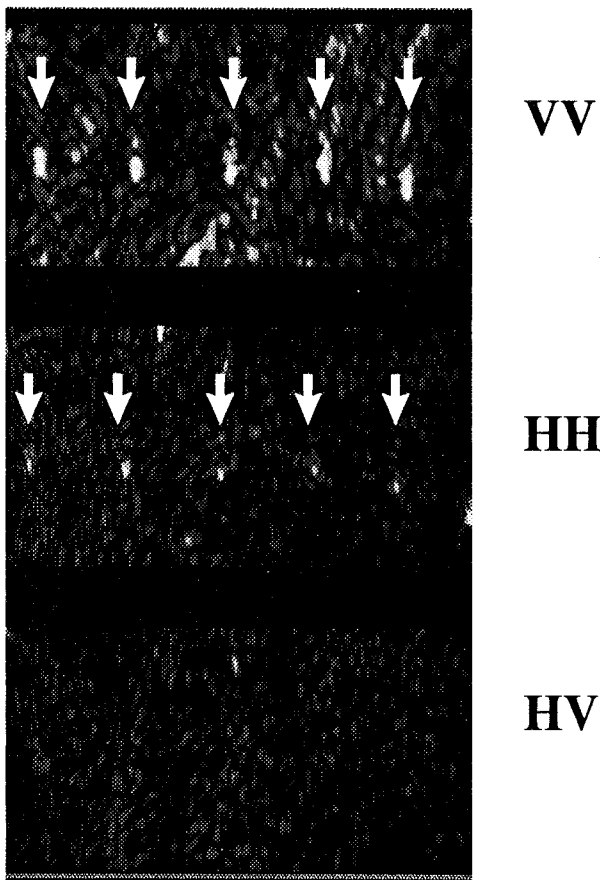


Fig. 3. SAR imagery for a row of five M20 mines buried 6 in (15.24 cm) deep, as measured by a UWB radar system. The three images correspond to VV-, HH-, and HV-polarizations, from top to bottom, and the mine locations are indicated by the arrows.

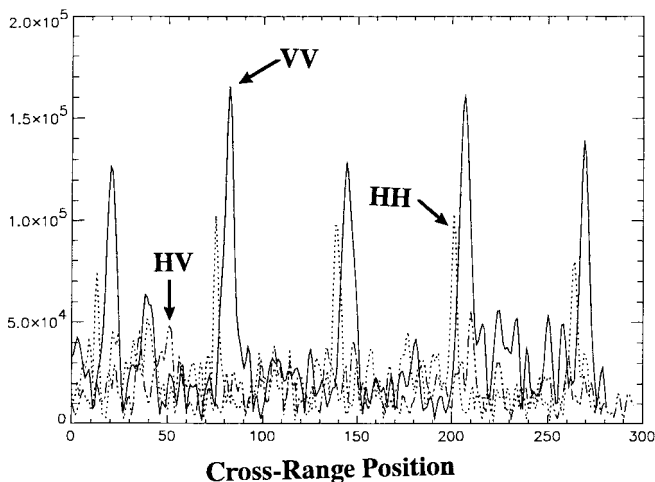


Fig. 4. Waveforms extracted by taking a "cut" out of the SAR imagery, in the cross-range direction, through the target centers. Results are shown for VV- (solid), HH- (dashed), and HV-polarizations (solid-dashed). The five peaks in the VV- and HH-polarizations correspond to the arrows in Fig. 3.

imagery gives a qualitative feel for the polarization dependence of the SAR imagery, we quantify such as follows. In Fig. 4 are plotted waveforms extracted from the SAR imagery, taking a cross-range "cut" in the image through the center of the mines (using knowledge of the actual target position). These data correspond to a 60° aperture

integration, over which the polarization of the transmitted radiation is approximately linearly polarized ($\pm 30^\circ$ about a line perpendicular to the synthetic aperture, along which the target center resides). We can see from these results—which were repeated faithfully for all M20 mines considered (as well as other BOR mines not shown)—that the copolarized component is significantly larger than its cross-polarized counterpart. Note from Fig. 2 that the M20 mine has small features that break the rigorous BOR symmetry, but appear to be unimportant for the wavelengths considered here. Note also that the VV and HH characteristics of the M20 mine are themselves different (although each is significantly stronger than the cross-polarized component); this issue has been explored in detail in a previous publication [10] and could be exploited in polarimetric mine detection.

II. CONCLUSION

In conclusion, we have explained theoretically that the backscattered fields from a BOR excited by a vertically or horizontally polarized plane wave are characterized by a zero cross-polarization component. These expectations have been confirmed experimentally using a UWB SAR system, considering anti-tank and anti-personnel mines that approximate BOR's (in addition to the M20, we considered the Valmara anti-personnel mine, results for which were not shown, for brevity). These polarimetric characteristics are valid, independent of the mine's electrical properties, as long as it satisfies the BOR model (i.e., they are valid for plastic and metal mines, although the measurements considered here were restricted to metal mines). Moreover, the soil can in general be continuously or discretely layered, as typically found in practice. Most natural and anthropic clutter do not satisfy the BOR model, and therefore, polarimetric SAR appears to be an effective tool for detection of an important and ubiquitous class of land mines. The principal limitation of this approach is the ability of electromagnetic waves to penetrate lossy soil; however, this is mitigated to some extent by the large integration afforded by the synthetic aperture (in contrast with conventional, local GPR systems [1]–[3], for which such integration gain is difficult to attain).

REFERENCES

- [1] L. Peters, J. J. Daniels, and J. D. Young, "Ground penetrating radar as a subsurface environmental sensing tool," *Proc. IEEE*, vol. 82, pp. 1802–1822, Dec. 1994.
- [2] G. S. Smith, "Directive properties of antennas for transmission into a material half-space," *IEEE Trans. Antennas Propagat.*, vol. AP-32, pp. 232–247, Feb. 1984.
- [3] P. J. B. Clarricoats, "Portable radar for the detection of buried objects," in *Proc. Radar 77 Inst. Elect. Eng. Conf.*, London, U.K., 1977.
- [4] M. A. Ressler and J. W. McCorkle, "Evolution of the Army Research Laboratory ultra-wideband test bed," in *Ultra-Wideband Short-Pulse Electromagnetics 2*, L. Carin and L. B. Felsen, Eds. New York: Plenum, 1995, pp. 109–123.
- [5] S. L. Earp, E. S. Hughes, T. J. Elkins, and R. Vickers, "Ultra-wideband ground-penetrating radar for the detection of buried metallic mines," *IEEE Aerosp. Eng. Syst. Mag.*, pp. 30–34, Sept. 1996.
- [6] A. C. Dubey, I. Cindrich, J. M. Ralston, and K. Rigano, Eds., *Detection Technologies for Mines and Minelike Targets*. Orlando, FL: SPIE, 1995, vol. 2496.
- [7] A. C. Dubey and R. L. Barnard, Eds., *Detection and Remediation Technologies for Mines and Minelike Targets*. Orlando, FL: SPIE, 1997, vol. 3079.
- [8] S. Vitebskiy and L. Carin, "Short-pulse plane wave scattering from a buried perfectly conducting body of revolution," *IEEE Trans. Antennas Propagat.*, vol. 44, pp. 112–120, Feb. 1996.
- [9] S. Vitebskiy, R. Sturgess, and L. Carin, "Late-time resonant frequencies of buried bodies of revolution," *IEEE Trans. Antennas Propagat.*, vol. 44, pp. 1575–1583, Dec. 1996.

- [10] S. Vitebskiy, L. Carin, M. Ressler, and F. Le, "Ultra-wideband, short-pulse ground-penetrating radar: Theory and measurement," *IEEE Trans. Geosci. Remote Sensing*, vol. 35, pp. 762–772, May 1997.
- [11] C. E. Baum and H. N. Kritikos, Eds., *Electromagnetic Symmetry*. New York: Taylor and Francis, 1995.
- [12] C. E. Baum, "Symmetry and electromagnetic scattering as a target discriminant," Phillips Lab., Interaction Note 523, Oct. 1996.

A Low-Frequency Radar Experiment for Measuring Vegetation Biomass

Marc L. Imhoff, Steven Carson, and Patrick Johnson

Abstract—Optical depth and backscatter measures were made at 18 frequencies between 50 and 450 MHz on two forest stands having dry biomass densities of 323 and 87 tons/ha to identify radar frequencies capable of penetrating heavy stands of vegetation. Good separation between stands was only achieved below 120 MHz.

Index Terms—Biomass measurement, forest stands, low-frequency radar, vegetation, VHF radar.

I. INTRODUCTION

Measuring the amount of carbon stored in the earth's dense tropical forests, in the form of biomass, has been an important part of efforts to quantify the exchange of carbon between the biosphere and atmosphere [1]. The amount of biomass stored in moist to wet tropical forest stands is considerable, with above-ground dry biomass densities in mature stands ranging from about 200 to 700 tons/ha [2]. Knowledge about both the biomass density and extent of the stands is important for estimating the amount of photosynthetically captured carbon stored in these stands on a regional and global basis.

A considerable investment has been made exploring the use of radar sensors to remotely measure vegetative biomass because of their ability to penetrate cloud cover and the way the transmitted electromagnetic radiation interacts with the physical structure of targets. Of particular interest has been the use of synthetic aperture radar (SAR) [3]–[5]. Many studies have reported correlations between radar backscatter and forest stand physical structural parameters that relate to biomass, such as height, basal area, and stocking density, and not surprisingly to stand biomass itself [6]–[10]. While these results are encouraging and SAR systems can be used to map biomass in some stands, saturation points, or the biomass level at which radar backscatter no longer increases with biomass for *P*-, *L*-, and *C*-band radar systems, have been reported as occurring at fairly low biomass loads. Saturation limits for a collection of coniferous forest stands using *P*-band (0.44 GHz), *L*-band (1.25 GHz), and *C*-band (5.3 GHz) SAR was reported to be at about 200 tons/ha for *P*-band and 100 tons/ha for *L*-band. No saturation limit was determined for

C-band [9]. Other work examining the saturation limits of some tropical forest stands and temperate coniferous stands, using the same SAR system, showed signal saturation limits with respect to biomass to be approximately 100 tons/ha for *P*-band, 40 tons/ha for *L*-band, and 20 tons/ha for *C*-band [11].

The exact location of these saturation limits and their effect on making biomass inventories has varied depending on the forest type and structure and whether polarimetric data were used. Smaller saturated forests, and some larger coniferous forests, can be successfully measured, as has been demonstrated by some (see [10]–[13] for temperate forests and [14]–[17] for tropical forests). Ultimately, however, the biomass saturation could still have a profound effect on global biomass inventories. An estimated 81% of the total terrestrial phytomass resides in forest stands with biomass densities above 100 tons/ha and nearly 41% in stands with densities above 200 tons/ha [11]. The growing awareness of the limitations presented by the saturation phenomenon has renewed interest in developing lower frequency radar systems to measure heavy biomass stands.

This paper describes initial results of an effort to explore the development of a low-frequency radar sensor to map biomass in heavy forest stands. The overall goal was to develop a radar sensor capable of operating at low frequencies and provide an inexpensive alternative to imaging radar systems. The work reported here is from the first phase. The work was carried out under NASA's Small Business Innovation Research Program (SBIR) with Zimmerman Associates, Inc./American Electronics, Inc. (ZAI/AMELEX), Vienna, VA, as the prime contractor for NASA's Goddard Space Flight Center, Greenbelt, MD. While the overall goal of this project (ongoing) is to develop an inexpensive system for measuring biomass in heavy stands, Phase I was primarily concerned with proof-of-concept and defining the limits of biomass saturation as a function of frequency from 450 (approximately *P*-band, which is the lower limit of NASA's current capability) to 50 MHz.

II. METHODOLOGY

In this first phase, a horizontal measurement geometry was used to conduct the tests (i.e., the direction of radar signal propagation was parallel with the ground). This geometry provided a convenient way to make low-cost, ground-based measurements as part of a feasibility study. However, this geometry creates interpretation problems when considering a synoptic perspective of canopy architecture. The dominant scatterers for this geometry are the tree trunks rather than the branches and leaves of the canopy, and this geometry represents a worst case for signal attenuation as a function of aspect angle at high-stocking densities. As such, these results could represent a lower bound on the saturation phenomenon as a function of frequency.

The horizontal viewing geometry used in this experiment requires the modeling of the backscatter from the forest as volumetric scatter because of the target's extent in range, as well as azimuth and elevation. Most of the radar data for biomass estimation in the literature are reported as surface scatter, in units of m^2 per m^2 , not volumetric scatter. The results reported here are reported in m^2 per m^3 because each radar range gate measures the radar reflectivity of the volume of trees, due to the measurement geometry. This prevents the direct comparison to data from previous studies.

The first objective of this work was to establish the frequency requirements for penetrating stands of heavy vegetation for this measurement geometry. The Phase I measurements were taken with vertically polarized radiating elements for practical measurement

Manuscript received May 12, 1997; revised December 17, 1997. This work was supported by NASA under Contract NAS5-32735.

M. L. Imhoff is with the Biospheric Sciences Branch, NASA Goddard Space Flight Center, Greenbelt, MD 20771 USA (e-mail: mimhoff@ltpmail.gsfc.nasa.gov).

S. Carson is with SAIC, Arlington, VA 22203 USA.

P. Johnson is with Zimmerman Associates, Inc., American Electronics, Inc., Vienna, VA 22182-2623 USA.

Publisher Item Identifier S 0196-2892(98)08278-3.